ORIGINAL ARTICLE

Cancer Science WILEY

VPS33B interacts with NESG1 to suppress cell growth and cisplatin chemoresistance in ovarian cancer

Yingxia Ning[1,2] | Zhaoyang Zeng[1] | Yuao Deng[3] | Weifeng Feng[4] | Lun Huang[2] |
Huiling Liu[2] | Jiazhi Lin[2] | Chen Zhang[5] | Yue Fan[6] | Longyang Liu[7] (iD)

[1]Department of Gynecology, the Integrated Hospital of Traditional Chinese Medicine, Southern Medical University, Guangzhou, China

[2]Department of Gynaecology and Obstetrics, The First Affiliated Hospital of Guangzhou Medical University, Guangzhou, China

[3]Department of Gynecology and Obstetrics, Shenzhen People's Hospital, Shenzhen, China

[4]The First Affiliated Hospital of Jinan University, Guangzhou, China

[5]Department of Clinical Pharmacy, Guangzhou First People's Hospital, Guangzhou, China

[6]Cancer Research Institute, Southern Medical University, Guangzhou, China

[7]Cancer Center, Integrated Hospital of Traditional Chinese Medicine, Southern Medical University, Guangzhou, China

Correspondence
Longyang Liu, Cancer Center, Integrated Hospital of Traditional Chinese Medicine, Southern Medical University, 13 Shiliugang ST, Guangzhou 510315, China.
Email: 13728035996@163.com

Yue Fan, Southern Medical University, Guangzhou, China.
Email: 258173709@qq.com

Abstract

The pathogenesis and cisplatin chemoresistance of ovarian cancer (OC) are still unclear. Vacuolar protein sorting-associated 33B (VPS33B) has not been reported in OC to date. In this study, immunohistochemistry was used to detect VPS33B protein expression between OC and ovarian tissues. MTT, EdU, colony formation, cell cycle, in vivo tumorigenesis, western blot, ChIP, EMSA, co-immunoprecipitation (CoIP), qRT-PCR, and microconfocal microscopy were used to explore the function and molecular mechanisms of VPS33B in OC cells. The results of the present study demonstrated that VPS33B protein expression was obviously reduced in OC compared with that in ovarian tissues. Overexpressed VPS33B suppressed cell cycle transition, cell growth, and chemoresistance to cisplatin in vitro and in vivo. Analysis of the mechanism indicated that overexpressed VPS33B regulated the epidermal growth factor receptor (EGFR)/PI3K/AKT/c-Myc/p53/miR-133a-3p feedback loop and reduced the expression of the cell cycle factor CDK4. Nasopharyngeal epithelium-specific protein 1 (NESG1) as a tumor suppressor not only interacted with VPS33B, but was also induced by VPS33B by the attenuation of PI3K/AKT/c-Jun-mediated transcription inhibition. Overexpressed NESG1 further suppressed cell growth by mediating VPS33B-modulated signals in VPS33B-overexpressing OC cells. Finally, NESG1 induced VPS33B expression by reducing the inhibition of PI3K/AKT/c-Jun-mediated transcription. Our study is the first to demonstrate that VPS33B serves as a tumor

---

suppressor, and VPS33B can interact with NESG1 to suppress cell growth and promote cisplatin sensitivity by regulating the EGFR/PI3K/AKT/c-Myc/p53/miR-133a-3p feedback loop in OC cells.

KEYWORDS
AKT, c-Myc, EGFR, miR-133a-3p, NESG1, PI3K, VPS33B

1 | INTRODUCTION

Ovarian cancer (OC) is the primary leading cause of cancer-related mortality among female reproductive malignant cancers in China.[1] Globally there are 239 000 new cases and 152 000 deaths every year.[2] With the development of new therapeutic approaches, the prognosis has improved, but the mortality remains very high.[3,4] The poor prognosis is due to high biological malignancy and cisplatin chemoresistance of OC cells.[5] Therefore, it is very valuable to investigate the mechanisms driving OC initiation and cisplatin chemoresistance, which may help to identify novel effective therapeutic approaches and improve the prognosis of OC patients.

VPS33B is a member of the Sec1 domain family, and it plays an important role in the segregation of intracellular molecules into distinct organelles.[6,7] VPS33B is necessary for megakaryocyte biogenesis, platelet activation, and in vivo thrombosis and homeostasis.[8,9] Previous reports have shown that it acts as a tumor suppressor in liver, nasopharyngeal, and colorectal cancer.[10-12] However, the role of VPS33B in OC has not been reported to date.

In a previous study, we cloned and revised NESG1, also referred to as CCDC19, in 1999 and 2005.[13,14] Our previous study demonstrated that NESG1 serves as a tumor suppressor, which can reduce cell growth, migration, and invasion in nasopharyngeal carcinoma (NPC), colorectal cancer, and non-small cell lung cancer.[12,15,16] However, the function and molecular mechanisms of NESG1 in OC have never been reported.

In this study, we explored the exact role of VPS33B in OC in vitro and in vivo. We found that VPS33B could interact with NESG1 to suppress cell growth and cisplatin chemoresistance by regulating the EGFR/PI3K/AKT/c-Myc/p53/miR-133a-3p feedback loop, which showed that VPS33B played a role as a tumor suppressor in OC.

2 | MATERIALS AND METHODS

2.1 | Tissues

Here, 137 epithelial OC tissues and 41 ovarian paraffin-embedded tissues were collected from the First Affiliated Hospital of Guangzhou Medical University. For the use of these clinical tissues, prior consent from the patients and approval from the Ethics Committees of this hospital were obtained. All tissues had confirmed pathological diagnosis.

2.2 | Immunohistochemistry

Paraffin sections (3 μm) from 137 OC and 41 ovarian tissues were carried out using immunohistochemistry (IHC) of VPS33B protein with anti-rabbit VPS33B antibody (1:100) (Proteintech Inc.) in accordance with the previous study.[14,17] Sections finally were visualized with 3,3′-diaminobenzidine (DAB) and counterstained with hematoxylin, mounted in neutral gum, and analyzed using a bright field microscope. The immunohistochemical staining sections were evaluated and scored separately by 2 pathologists as previously described.[18,19] For statistical analysis, final scores of 0-5 or 6-7 were, respectively, considered to be low and high expression.

2.3 | Cell culture

Both OVCAR-3 and SKOV-3 cell lines were purchased from the Cell Bank of Type Culture Collection of Chinese Academy of Sciences (Shanghai, China). SKOV-3 was cultured in McCoy's 5a (modified) medium (Gibco, Thermo Fisher Scientific) supplemented with 10% FBS (ExCell). OVCAR-3 was cultured in RPMI 1640 medium (HyClone) supplemented with 20% FBS (ExCell). Both cell lines were grown in a humidified chamber with 5% CO_2 in air at 37℃.

2.4 | Lentivirus production and infection

Lentiviral particles carrying the Gv-VPS33B precursor and its flanking control sequence were constructed using the GeneChem kit. OVCAR-3 and SKOV-3 cells were transfected with a lentiviral vector, and polyclonal cells with green fluorescent protein signals were selected for further experiments.

2.5 | Reverse transcription-quantitative polymerase chain reaction

RNA isolation, reverse transcription, and RT-qPCR were performed in OC cell lines as described in a previous study.[19,20] Specific sense primers of VPS33B, miR-133a-3p, and GAPDH are listed in Supplementary Table S1.

2.6 | Cell proliferation analysis

Cell proliferation was analyzed using the MTT assay as described in a previous study.[20,21] Experiments were done in triplicate.

2.7 | Colony formation assay

Colony formation assay was analyzed in accordance with a previous description.[22] Experiments were done in triplicate.

2.8 | Cell cycle analysis, EdU incorporation assays

Cell cycle analysis and EdU incorporation assay were performed as described in a previous study.[18] Each experiment was done in triplicate.

2.9 | In vivo studies

For in vivo tumorigenesis assays, in total 1×10^7 OVCAR-3 or SKOV-3 cells overexpressing VPSS33B and their negative control cells in 0.1 mL PBS were subcutaneously injected into the left or right flank of female BALB/c nude mice ($N = 5$) aged 4 wk. All animal studies were conducted in accordance with the principles and procedures of the Southern Medical University Guide for the Care and Use of Animals. The weight of the implantation tumor was finally determined when the tumor grew to 30 d.

2.10 | Transient transfection

siRNAs (including NC: negative control) and miR-133a-3p mimics were synthesized by RiboBio Inc. We constructed the VPS33B and NESG1 plasmid (including NC). Approximately 12 h prior to transfection, OVCAR-3 and SKOV-3 cells were seeded onto a 6-well plate (Nest, Biotechnology Co., Ltd, China) at 40%-60% confluency. siRNA, plasmid, and miRNA mimics were then transfected at a working concentration of 100 nM using TurboFect siRNA Transfection Reagents (Fermentas, Vilnius, Lithuania). Cells were collected after 48-72 h. The sequences are listed in Table S2.

2.11 | Western blot analysis

Western blot analysis was conducted as described in a previous study.[22] The antibodies included anti-VPS33B, EGFR, PI3K, AKT, pPI3K, pAKT, c-Myc, P-gp/ABCB1, ABCG2, p53, CDK4, GADPH, and β-actin antibody. Images were captured with MiniChemi, Beijing Sage Creation Science, Co. Ltd., Beijing, China). The antibodies are listed in Table S3.

2.12 | Co-immunoprecipitation assay

We transfected OVCAR-3 and SKOV-3 cells with the VPS33B plasmid carrying an HA flag and the NESG1 plasmid carrying an MYC flag. We obtained immunoprecipitation (IP) proteins in accordance with the instructions provided by the manufacturer of the Thermo Fisher Co-IP kit. After sodium dodecyl sulfate polyacrylamide gel electrophoresis and image capturing, we examined the interaction between NESG1and VPS33B.

2.13 | Electrophoretic mobility shift assay

Electrophoretic mobility shift assay was conducted using an EMSA kit (BersinBio, Guangzhou, China). Nuclear extracts were obtained from the cells, and the concentration was determined using a BCA assay kit. EMSA assay was performed in a reaction mixture containing nuclear extracts and biotin-labeled probes. After electrophoresis and incubation, signals were recorded and analyzed. The sequences used in EMSA assay are listed in Table S4.

2.14 | Confocal laser assay

Based on the cell slide assay, we transfected OVCAR-3 cells with the VPS33B plasmid and the NESG1 plasmid in a 6-well plate. After 48 h, the cells were immobilized with 4% paraformaldehyde. In accordance with the instructions for immunofluorescence staining, we obtained our slide with double fluorescence labeling. Antibodies, including anti-HA and MYC, were diluted at 1:100, and secondary fluorescent antibodies 488 and 573 were diluted at 1:500 (Bioworld Technology, Inc). Images were captured using a laser scanning confocal microscope (ECLIPSI-Ti, Nikon).

2.15 | Chromatin immunoprecipitation

The combinations of p53 with miR-133a-3p, c-Myc with p53, and c-Jun with NESG1 or VPS33B were confirmed using ChIP assay. Cells were transfected with p53, c-MYC, or c-Jun plasmids and then fixed with 1% formaldehyde. In accordance with the instructions provided with the ChIP assay kit (Thermo Fisher, Inc, China), crosslinked DNA was sheared to 200-1000 base pairs in length with sonication and then subjected to immunoselection. RT-qPCR was used to measure the enrichment of DNA fragments at the putative p53 binding site in miR-133a-3p, c-Myc binding site in p53, and c-Jun binding site in the NESG1 or VPS33B promoter based on specific primers. The specific ChIP primers are listed in Table S1.

2.16 | Luciferase report activity

Target gene promoter vectors including pGL3.0 (wt), pGL3.0 (mt) of miR-133-3p, p53, NESG1, and VPS33B were constructed. The
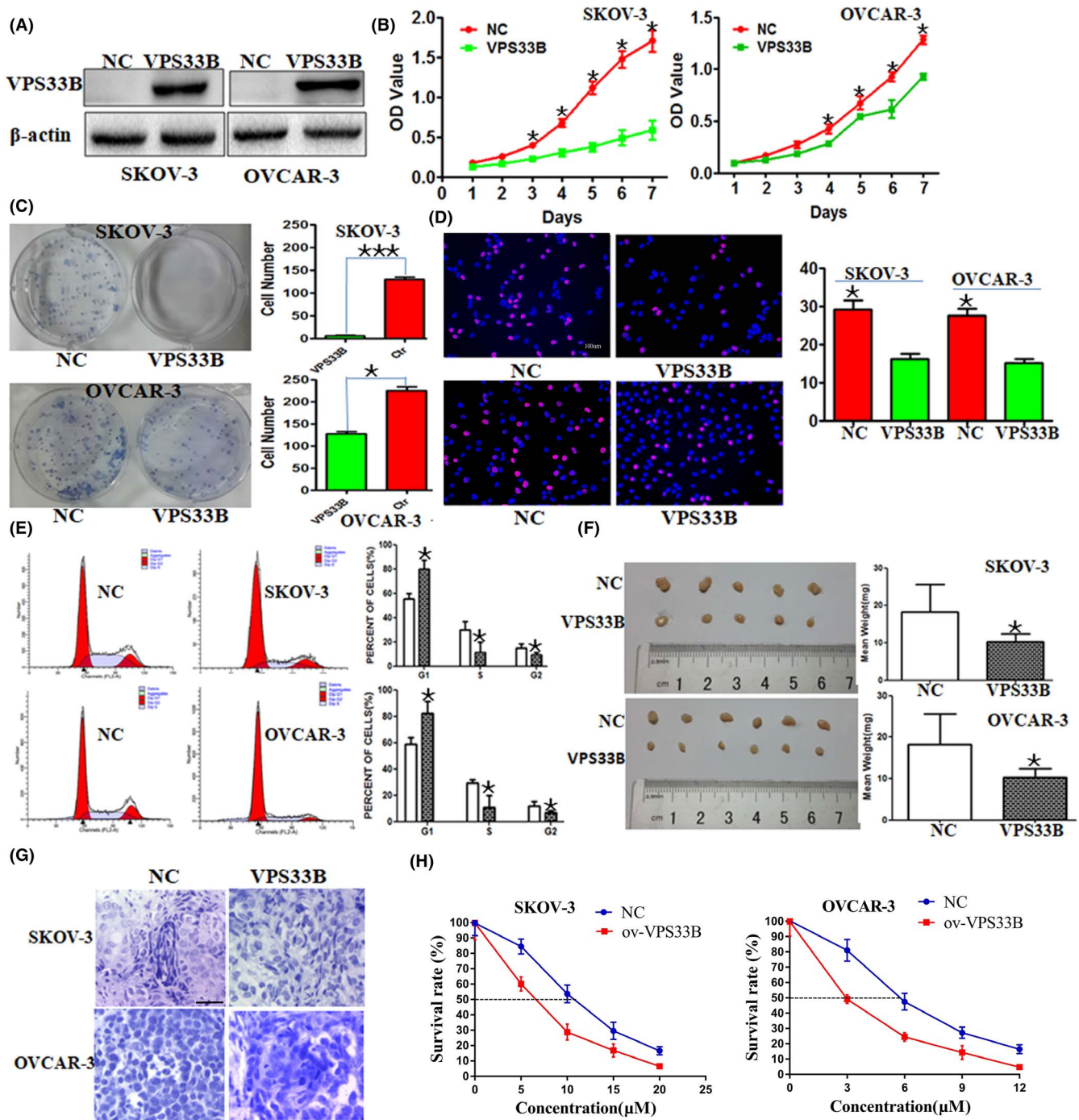
FIGURE 1 VPS33B overexpression inhibits OC cell proliferation in vitro and in vivo. A, SKOV-3 and OVCAR-3 cells were transfected with GV-VPS33B or empty vectors. Efficiency of overexpression was measured using western blot analysis. *P <.05. B-F, The in vitro function of VPS33B was measured using MTT assay (B), colony-forming assay (C), EdU assay (×100 magnification; scale bar, 200 μm) (D), and flow cytometry assay (E) in SKOV-3-Gv-VPS33B and OVCAR-3-Gv-VPS33B cells. F, Implantation tumors of SKOV-3-Gv-VPS33B and OVCAR-3-Gv-VPS33B cells or controls after 12 d. G, Hematoxylin and eosin staining of implantation tumors in SKOV-3-Gv-VPS33B and OVCAR-3-Gv-VPS33B cells (×400 magnification; scale bar, 50 μm). H, cisplatin sensitivity was evaluated in SKOV-3-Gv-VPS33B and OVCAR-3-Gv-VPS33B cells. Experiments were repeated 3 times, obtaining similar results. Error bars represent mean ± SD, *P <.05, ***P <.001

pGL3.0 vector was used as the negative control. Furthermore, pcDNA 3.1 vectors, respectively, containing transcription factor of p53, c-Myc, and c-Jun were bought from Shanghai Genechem Co., Ltd., China. pcDNA3.1 was used as the control. Vectors, respectively,

were transfected into SKOV-3 and OVCAR-3 cells. Luciferase activity was measured using the Dual-Luciferase Reporter Assay System (Promega Corporation) 48 h after transfection. Data were collected, and the ratio of luciferase activity was calculated.

2.17 | In vitro cisplatin treatment experiment

Drug sensitivity test was detected by the MTT assay. Cells were seeded in 96-well plates at a density of 2×10^3 cells/well and treated with 0, 5, 10, 15, 20 (SKOV-3) or 0, 3, 6, 9, 12 μM (OVCAR-3) cisplatin (Qilu Pharmaceutical Co., Ltd.) for 48 h. Subsequently, 20 μL of MTT (5 mg/mL; Sigma-Aldrich) was added to each well and incubated at 37°C for 4 h. Then supernatants were removed and 150 μL of DMSO (Sigma-Aldrich) was added to measure the absorbance value (OD) of each well at 490 nm. The calculated rates were used for curve fitting and calculation of IC_{50}. Experiments were performed 3 times.

2.18 | Statistical analysis

All data represented at least triplicate samples. IBM SPSS 21.0 (IBM Corporation) and GraphPad Prism 7.0 (GraphPad Software, Inc) software were used for statistical analysis. Data were presented as mean ± SEM. One-way ANOVA or two-tailed Student t test was used for comparison between groups. All of $P < .05$ were considered statistically significant.

3 | RESULTS

3.1 | Immunohistochemistry

IHC showed that VPS33B protein expression was located at cytoplasm (Figure S1). Furthermore, we found that in 75.4% (31/41) of ovarian tissues, VPS33B protein was highly expressed. In comparison, only 51.1% (70/137) of OC tissues had highly expressed, which is significantly lower than that in ovarian samples ($P < .001$).

3.2 | Overexpressed VPS33B inhibits OC cell proliferation in vitro and in vivo by regulating EGFR/PI3K/AKT/c-MYC pathway

To test the function of VPS33B in vitro, we transfected a lentivirus carrying the VPS33B cDNA into OVCAR-3 and SKOV-3 cell lines to establish OVCAR-3-Gv-VPS33B and SKOV-3-Gv-VPS33B stable cell lines. Western blot assay indicated significantly upregulated VPS33B expression (Figure 1A). MTT assay showed that VPS33B overexpression statistically decreased cell proliferation relative to the negative control cells (Figure 1B). Colony formation assay verified the inhibition of cell growth by VPS33B (Figure 1C). EdU assay (Figure 1D) and flow cytometry (FCM) (Figure 1E) indicated that VPS33B blocked the G1 to S cell cycle transition. Consistent with the assays in vitro, the nude mice subcutaneous tumor formation results showed that VPS33B overexpression inhibited cell proliferation in vivo (Figure 1F). Figure 1G showed the hematoxylin and eosin staining results of subcutaneous tumors in VPS33B-overexpressed cells. Moreover, we treated OVCAR-3-Gv-VPS33B, SKOV-3-Gv-VPS33B, or their controls with a concentration gradient of cisplatin. The IC50

value for overexpressed VPS33B cells was statistically lower than those of the controls (Figure 1H). In addition, to confirm the inhibition of VPS33B, we transfected VPS33B-siRNAs or control into overexpressed VPS33B OC cells. RT-qPCR and western blot analysis were conducted to detect their interfering efficiency (Figure S2A, B). MTT assay (Figure S2C) and EdU assay (Figure S2D) revealed that VPS33B interference could rescue cell growth.

Moreover, to determine the mechanism of VPS33B in OC, we analyzed its related pathways. The results showed that overexpressed VPS33B could decrease the expression of EGFR, PI3K/AKT, c-MYC, P-gp, ABCG2, and the downstream cell cycle factor CDK4. In contrast, the cell cycle inhibitor p53 was upregulated (Figure 2).

3.3 | miR-133a-3p inactivates EGFR/PI3K/AKT/c-Myc signaling to suppress cell proliferation, invasion, and migration in OC

We transfected OVCAR-3 and SKOV-3 cells with miR-133a-3p mimics and measured the efficiency of transfection using RT-qPCR (Figure S3A). MTT and EdU assays showed that overexpressed miR-133a-3p reduced cell growth and cell cycle arrest in OC cells (Figure S3B,C). Western blot assay showed that miR-133a-3p decreased the EGFR/PI3K/AKT/c-Myc pathway and the downstream cell cycle factor CDK4, as well as upregulated p53 (Figure S3D).
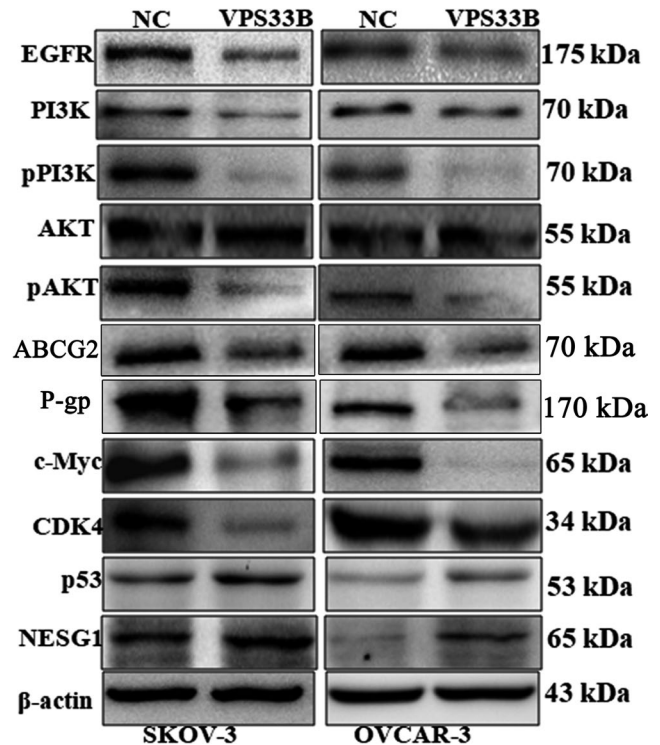

FIGURE 2 VPS33B regulates EGFR/PI3K/AKT/c-Myc signaling and downstream cell cycle and epithelial-mesenchymal transition (EMT) factors. Levels of EGFR, PI3K/AKT, pPI3K/AKT, c-MYC, P-gp, ABCG2, c-Jun, CDK4, and p53 were measured using western blot analysis after VPS33B overexpression, with β-actin as the inner control

3.4 | p53 inactivates EGFR/PI3K/AKT/c-Myc pathway by binding to the miR-133a-3p promoter in OC cells

We used the University of California, Santa Cruz (UCSC) genome browser (http://genome.ucsc.edu/) and the ALGGEN PROMO (http://alggen.lsi.upc.es/cgi-bin/promo_v3/promo/promoinit. cgi?dirDB=TF_8.3) software to search a candidate upstream

transcription factor of miR-133-3p, and we found that p53 may bind to the miR-133a-3p promoter region (−1234 to c. −1228: TAACGGG) and precursor (Figure 3A). mRNA expression of miR-133a-3p was increased after p53 transfection as shown by RT-qPCR (Figure 3B). ChIP and EMSA both confirmed that p53 could directly bind to the miR-133a-3p promoter in OC cells (Figure 3C-E). Luciferase reporter activity demonstrated that p53 could increase miR-133a-3p activity (Figure 3F).
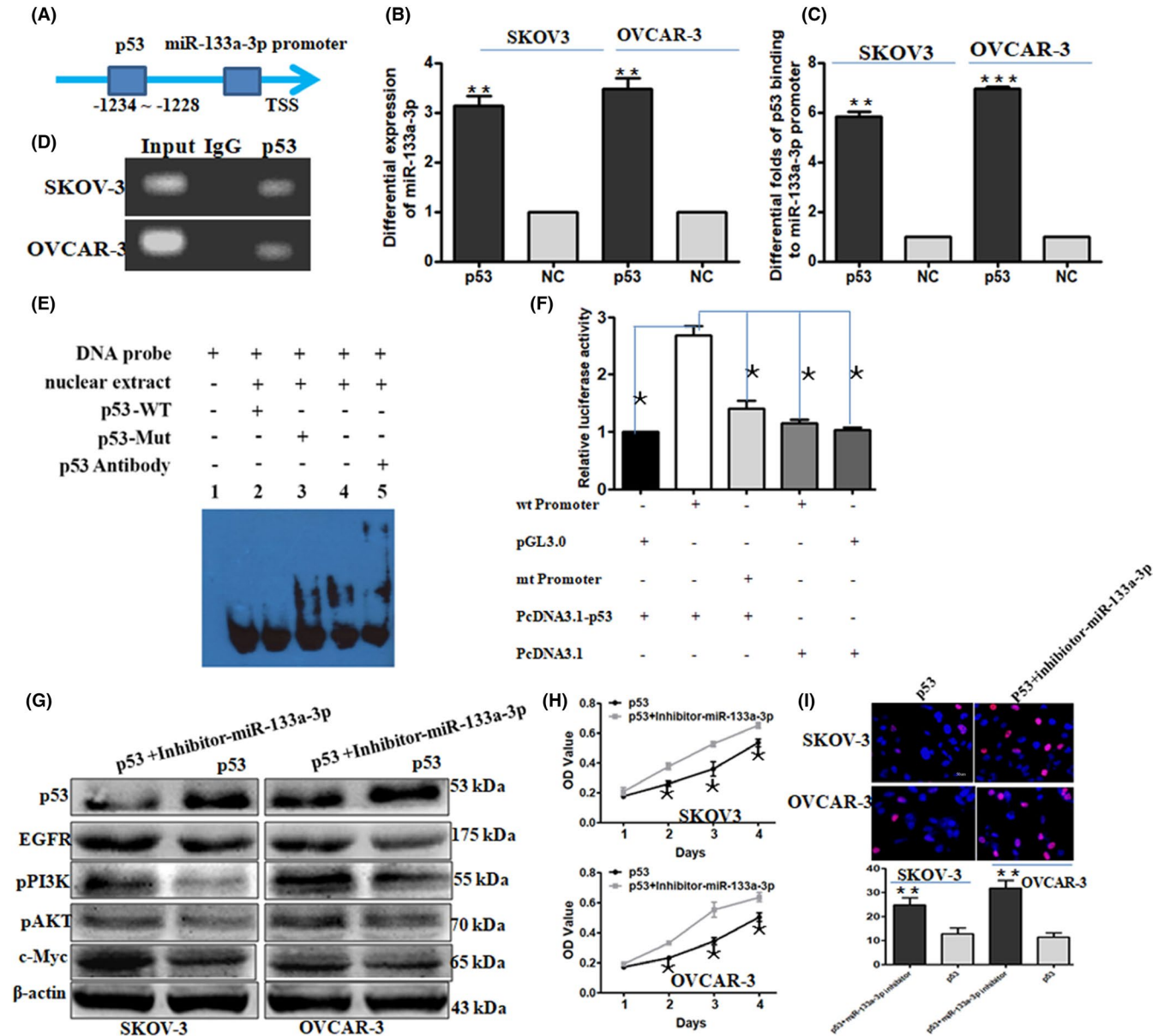

FIGURE 3 p53 inactivates EGFR/PI3/AKT/c-Myc signaling by directly simulating miR-133a-3p. A, Schematic of the promoter regions of miR-133a-3p with the putative p53 transcription binding site. B, Expression levels of miR-133a-3p after p53 overexpression in OC cells were determined using RT-qPCR. C, The combination of p53 with the miR-133a-3p promoter was examined using real-time PCR. D, PCR gel showing amplification of p53-binding sites after ChIP using antibody against p53. E, EMSA result from nuclear proteins extracted from SKOV-3 cells after incubation with individual biotin-labeled probes. Lane 1 to Lane 5 correspond to the negative control, WT competition group, MT competition group, treatment group, and supershift group. F, p53 induced miR-133a-3p promoter activity using luciferase report assay. G, Changes in EGFR, pPI3/AKT, c-Myc, and p53 expression were detected using western blot analysis after transfection of the miR-133a-3p inhibitor in p53-overexpressed OC cells. H, I, MTT and EdU (×400 magnification; scale bar, 50 μm) assays were used to measure changes in cell proliferation and cell cycle transition after transfection of the miR-133a-3p inhibitor in p53-overexpressed OC cells. Mean ± SD, *P <.05,**P <.01, ***P <.001

To verify the exact role of p53/miR-133a-3p in OC cells, miR-133a-3p inhibitor was transfected to p53-overexpressed OC cell lines. The findings showed upregulation of EGFR/PI3K/AKT/c-Myc signaling and downregulation of p53 after transfection (Figure 3G). Cell growth and EdU staining were clearly reversed in p53-overexpressed OC cells after transfection (Figure 3H, I).

3.5 | c-Myc feedbacks miR-133a-3p/EGFR/ PI3K/ AKT signaling by regulating p53

When c-Myc was overexpressed, the mRNA levels of p53 in OC cells were downregulated (Figure 4A). Results of bioinformatics software prediction showed that c-Myc may bind to the promoter of p53 (Figure 4B). ChIP and luciferase activity assays indicated that c-Myc
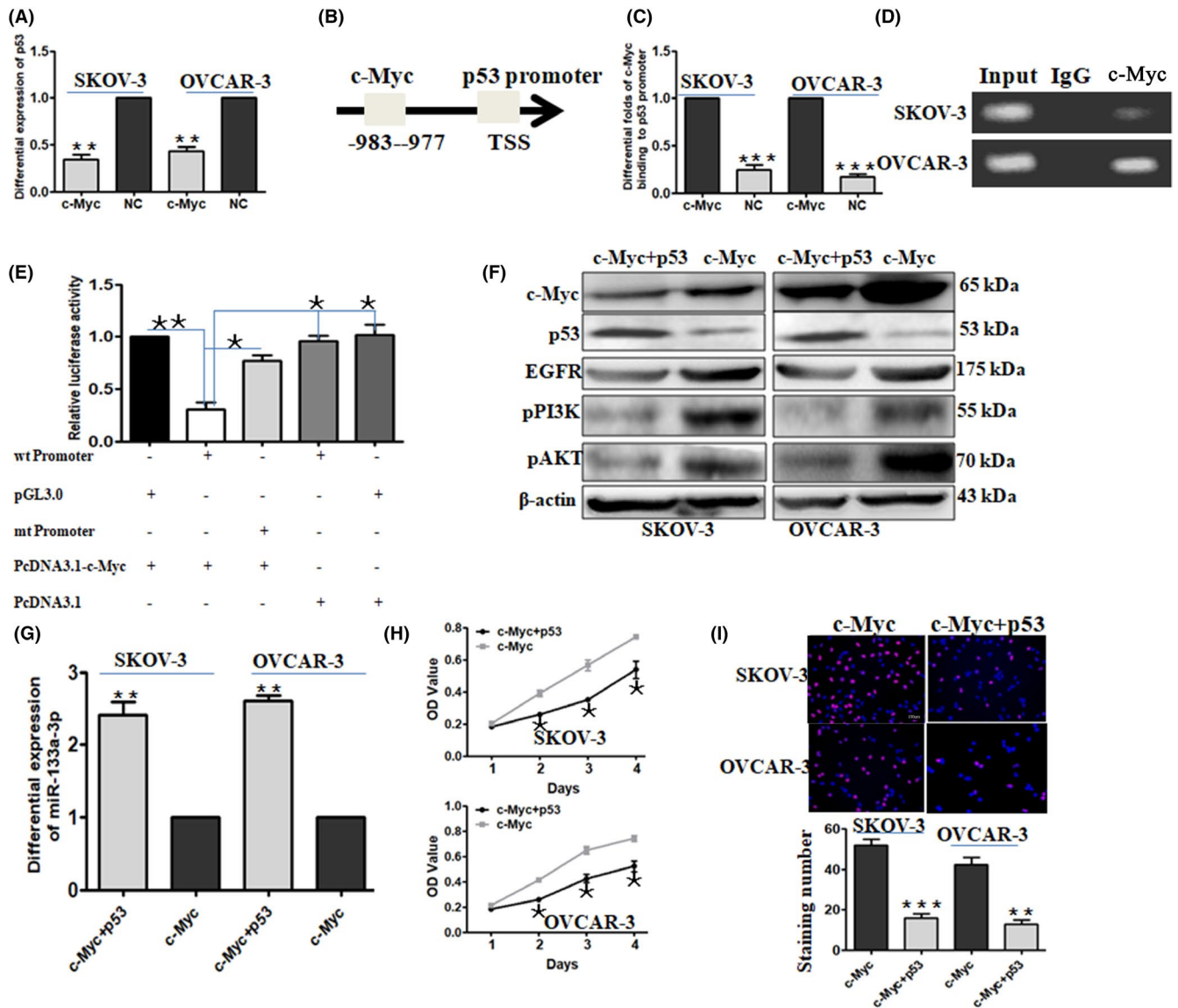

FIGURE 4 c-Myc feedbacks miR-133a-3p/EGFR EGFR/PI3K/AKT signaling by modulating p53. A, mRNA levels of p53 after interference of c-Myc measured by RT-qPCR. B, Schematic of the promoter regions of p53 with putative c-MYC TFBS. C, D, RT-qPCR and gel electrophoresis showed the combination of c-MYC with the p53 promoter using ChIP and antibody against c-Myc. E, Relative luciferase activity of the p53 promoter in SKOV-3 and OVCAR-3 cells after transfection of c-Myc plasmids. F, Expression levels of c-Myc, EGFR, pPI3K/AKT, and p53 were detected using western blot analysis after transfection of the p53 plasmid into c-Myc-overexpressed SKOV-3 and OVCAR-3 cells, with β-actin as controls. G, Expression levels of miR-133a-3 were measured using RT-qPCR after overexpression of the p53 plasmid in c-Myc-overexpressed SKOV-3 and OVCAR-3 cells. H, I, MTT and EdU (×100 magnification; scale bar, 200 μm) assays were used to measure changes in cell proliferation and cell cycle transition after transfection of p53 plasmid in c-Myc-overexpressed OC cells. Mean ± SD,*P <.05,**P <.01, ***P <.001

directly combined to the promoter of p53 and reduced its activity in OC cells (Figure 4C-E). In addition, transfection of p53 plasmid in c-Myc-overexpressed OC cells not only suppressed EGFR/PI3K/AKT/c-Myc signaling and upregulated miR-133a-3p expression (Figure 4F, G), but also reduced cell growth and EdU staining (Figure 4H, I).

3.6 | EGFR feedback downregulates miR-133a-3p through the PI3K/AKT/c-Myc/p53 pathway

Transfecting EGFR plasmid (pcDNA 3.1 + EGFR cDNA) into OC cells showed that the EGFR/PI3K/AKT/c-Myc signal was significantly up-regulated (Figure S4A). In addition, the expression levels of p53 and

miR-133a-3p were significantly downregulated, as shown by west-ern blot or RT-qPCR (Figures S4A, B). ChIP assay showed that the combination of p53 with the miR-133a-3p promoter was decreased following EGFR overexpression (Figure S4C).

3.7 | VPS33B regulates EGFR/PI3K/AKT/c-Myc/p53/miR-133a-3p signal

To determine whether miR-133a-3p was involved in VPS33B-regulated EGFR/PI3K/AKT/c-Myc/p53 signaling and formed a feedback loop in OC cells, we detected the mRNA expression of miR-133a-3p in VPS33B-overexpressed cells using RT-qPCR.
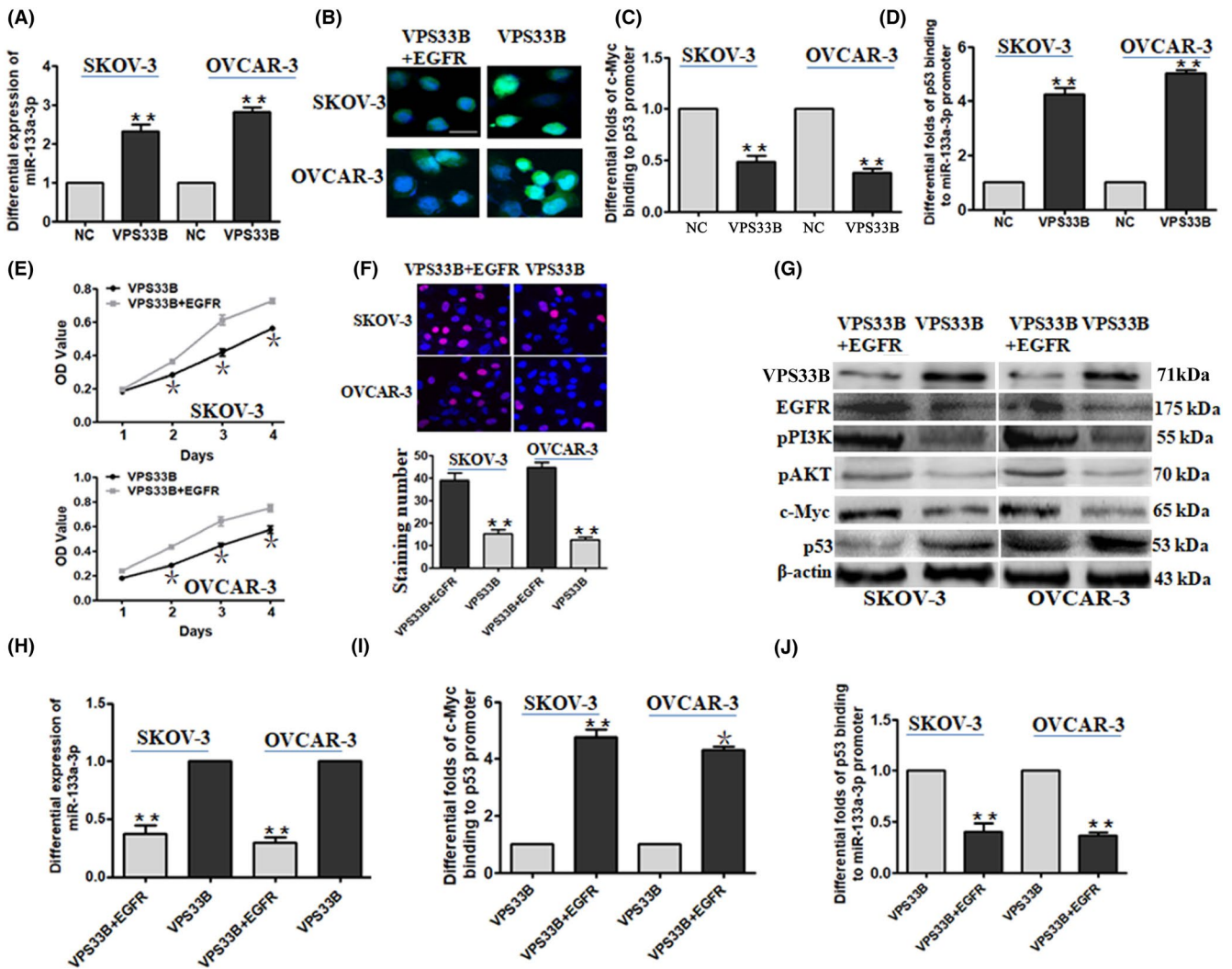

FIGURE 5 VPS33B modulates the feedback loop of EGFR/PI3K/AKT/c-Myc/P53/miR-133a-3p by upregulating miR-133a-3p. A, Expression level of miR-133a-3p was measured after VPS33B overexpression using RT-qPCR. B, Confocal laser assay confirmed the nuclear translocation of p53 in VPS33B-overexpressed cells (×630 magnification; scale bar, 50 μm). Cells were stained with RED for p53 and DAPI to label nuclear DNA. C, The combination of c-Myc with the p53 promoter was measured using ChIP assay in VPS33B overexpressed cells. D, The combination of p53 with the miR-133a-3p promoter was measured using ChIP assays in VPS33B-overexpressed cells. E, F, Transduction of EGFR reversed cell proliferation and EdU (×400 magnification; scale bar, 50 μm) staining in VPS33B-overexpressed OC cells. G, H, EGFR overexpression upregulated PI3K/AKT/c-Myc expression and decreased the p53/miR-133a-3p signal in VPS33B-overexpressed OC cells. I, J, Transduction of EGFR increased the combination of c-Myc with the p53 promoter and decreased the combination of p53 with the miR-133a-3p promoter in VPS33B-overexpressed OC cells. Mean ± SD, *P <.05,**P <.01

Results showed that VPS33B upregulated the expression of miR-133a-3p (Figure 5A). Confocal laser assay indicated that over-expressed VPS33B increased nuclear translocation of p53 after VPS33B was overexpressed in OC cells (Figure 5B). The combination of c-Myc with the p53 promoter was markedly decreased (Figure 5C). Inversely, the combination of p53 with the miR-133a-3p promoter was significantly increased (Figure 5D). Furthermore, EGFR cDNA transfection not only promoted cell growth and EdU staining (Figure 5E, F), but also increased PI3K/AKT/c-Myc signaling and decreased the expression of p53 and miR-133a-3p in VPS33B-overexpressed cells (Figure 5G, H). Finally, the combination of c-Myc with the p53 promoter was markedly increased, and the combination of p53 with the miR-133a-3p promoter was markedly decreased in VPS33B-overexpressed cells after transfection with the pcDNA3.1-EGFR plasmid (Figure 5I, J).

3.8 | VPS33B interacts with NESG1 in OC cells

In a previous study, using the yeast-two-hybrid (Y2H) technique, we detected that VPS33B may interact with NESG1.[11] To determine the interaction, we transfected OC cells with the VPS33B plasmid (HA flag) and NESG1 plasmid (MYC flag). CoIP assay demonstrated the interaction between VPS33B and NESG1 (Figure 6A, B) in OVCAR-3 cells. Confocal laser analysis confirmed that both VPS33B and NESG1 were located in the cytoplasm (Figure 6C).

3.9 | VPS33B induces NESG1 expression by attenuating the EGFR/PI3K/AKT/c-Jun pathway

Overexpressed VPS33B resulted in NESG1 upregulation on mRNA level in OC cells (Figure 7A). The UCSC and PROMO software were used to predict transcription factors that may bind to the NESG1 promoter, and the results showed that c-Jun was a candidate transcription factor (Figure 7B). mRNA and protein levels of NESG1

decreased after c-Jun plasmid transfection (Figure 7C, D). In addition, we demonstrated the combination of c-Jun with the NESG1 promoter with ChIP assay (Figure 7E, F). Moreover, luciferase report assay confirmed that c-Jun could directly reduce NESG1 expression by binding to its promoter (Figure 7G).

Finally, EGFR plasmid transfection in VPS33B-overexpressed cells increased the expression of PI3K/AKT/c-Jun signals (Figure 7H), reduced the NESG1 expression (Figure 7I), and increased the combination of c-Jun with NESG1 (Figure 7J). These results showed that VPS33B induced NESG1 expression by attenuating the EGFR/PI3K/AKT/c-Jun pathway.

3.10 | NESG1 mediates VPS33B-suppressing malignant phenotypes by regulating the EGFR/PI3K/AKT /c-Myc/p53/miR-133a-3p feedback loop

To explore the exact role of NESG1 in OC, NESG1 plasmid and control vectors were transfected into VPS33B-overexpressing OC cells, respectively. We performed MTT and EdU assay and found that increased NESG1 inhibited cell proliferation and EdU staining in OC (Figure S5A, B).

To demonstrate whether NESG1 also modulates the EGFR/PI3K/AKT/c-MYC/p53/miR-133a-3p feedback loop, we transfected OC cells with the NESG1 plasmid in VPS33B-overexpressed OC cells, and then found a decrease in the expression of EGFR, PI3K/AKT, c-Myc, c-Jun, and cell cycle factor CDK4 using western blot assay (Figure S5C). We simultaneously detected increased expression of p53, and miR-133a-3p after NESG1 overexpression by western blot analysis and RT-qPCR (Figure S5C, D). Finally, we observed that the combination of c-Myc with the p53 promoter was decreased, and the combination of p53 with the miR-133a-3p promoter was increased (Figure S5E, F). These findings suggest that NESG1 mediated the suppression of VPS33B in OC cell proliferation by regulating the EGFR/PI3K/AKT /c-Myc/p53/miR-133a-3p feedback loop.
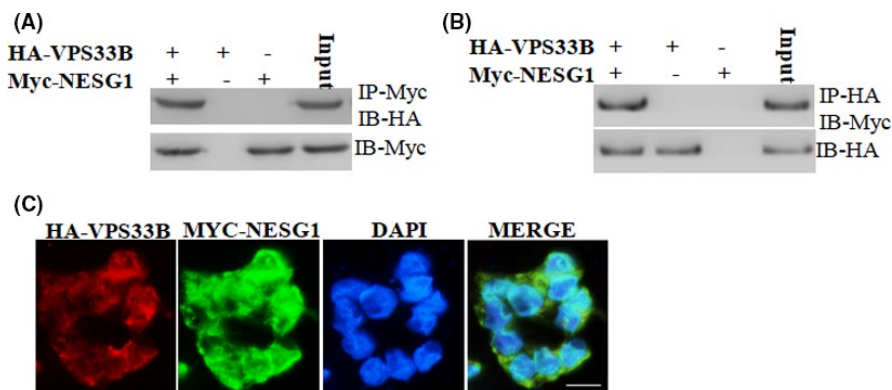

FIGURE 6 VPS33B interacts with NESG1 in OC cells. A, B, SKOV-3 cells were transfected with VPS33B plasmid-carried HA flag and NESG1 plasmid-carried MYC flag. Co-immunoprecipitation assay was used to prove the interaction between VPS33B and NESG1. C, Relationship between VPS33B and NESG1 was confirmed using a confocal laser (×630 magnification; scale bar, 25 μm). VPS33B-HA stained with red fluorescence and NESG1-MYC with green and nuclear DAPI fluorescence
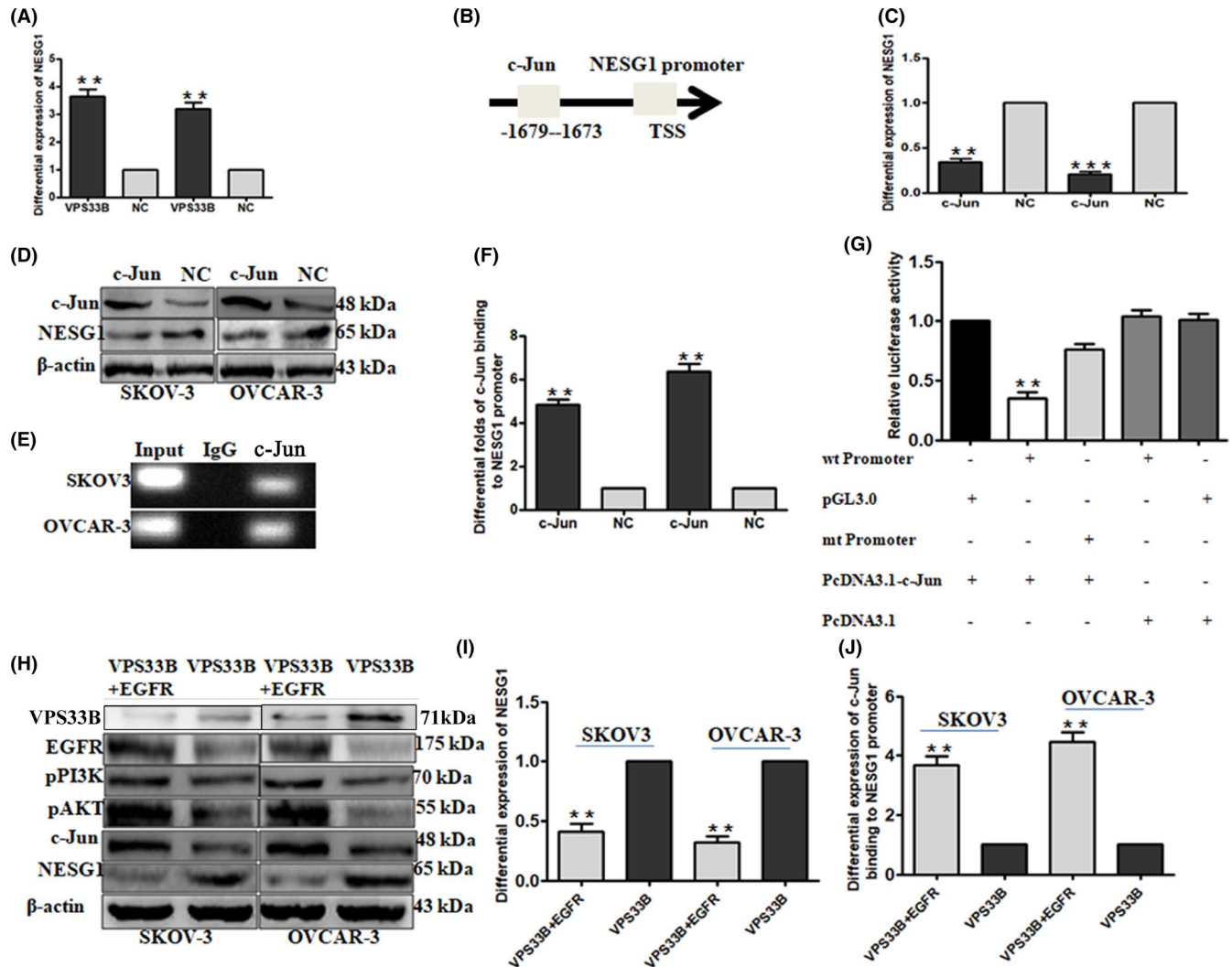
FIGURE 7 VPS33B induces NESG1 expression by downregulating PI3K/AKT/c-Jun. A, VPS33B stimulated NESG1 expression in mRNA level. B, c-Jun as a transcription factor was predicted to bind to NESG1 promoter. C, D, c-Jun overexpression downregulated NESG1 mRNA and protein levels. E, F, c-Jun combined with the NESG1 promoter using ChIP and RT-qPCR and gel electrophoresis assays. G, Relative luciferase activity of the NESG1 promoter in SKOV-3 and OVCAR-3 cells after transfecting c-Jun plasmids. H, EGFR overexpression upregulated the expression of the PI3K/AKT/c-Jun signal and reduces NESG1 expression in VPS33B-overexpressed OC cells using western blot assay. I, NESG1 mRNA expression was significantly reduced after transfection of EGFR plasmid into VPS33B-overexpressing OC cells. J, Overexpressing EGFR increased the combination of c-Jun with the NESG1 promoter in VPS33B-overexpressed OC cells. Mean ± SD, **$P <.01$, ***$P <.001$

3.11 | NESG1 induces VPS33B expression by attenuating the EGFR/PI3K/AKT pathway

Overexpressed NESG1 led to VPS33B increasing in mRNA level of OC cells (Figure S6A). UCSC and PROMO software were used to predict candidate transcription factors binding to the VPS33B promoter and found c-Jun was a candidate potential factor (Figure S6B). Both mRNA and the protein levels of VPS33B were reduced after c-Jun plasmid transfection (Figure S6C, D). ChIP assay demonstrated the combination of c-Jun with the VPS33B promoter (Figure S6E, F). Luciferase report assay confirmed that c-Jun could directly reduce the activity of the VPS33B promoter by binding to its promoter (Figure S6G).

EGFR overexpression in NESG1-overexpressed cells led to increased PI3K/AKT/c-Jun expression (Figure S6H), reduced VPS33B mRNA and protein levels (Figure S6H, I), and increased the combination of c-Jun with the VPS33B promoter (Figure S6J). These results showed that NESG1 induced VPS33B expression by attenuating the EGFR/PI3K/AKT/c-Jun pathway.

4 | DISCUSSION

In this study, we detected the protein level of VPS33B in OC and ovarian tissues for the first time. The data showed that VPS33B was located in the cytoplasm and VPS33B expression

was obviously downregulated in OC tissues compared with ovarian tissues. This result suggests that VPS33B may participate in the pathogenesis of OC. Functional studies further showed that overexpressed VPS33B inhibited cell proliferation in vitro and in vivo and suppressed cisplatin chemoresistance in OC. Cell cycle transition is a vital factor promoting cancer cell proliferation and inducing chemotherapeutic resistance to cisplatin,[23,24] and P-gp and ABCG2 are both the biomarkers of chemotherapeutic resistance. EGFR is a receptor of the epidermal growth factor family. Activated EGFR promotes cell proliferation and pathogenesis of various tumors.[11,12] EGFR is a key factor that can activate the PI3K/AKT pathway,[25] an upstream oncogenic signal of cell cycle transition and c-Jun in various tumors. In previous studies,[11,12] we reported that VPS33B overexpression suppressed the expression of c-MYC, CDK4, and increased p53 expression. Consistent with our previous reports,[11,12] we found that in OC cells VPS33B overexpression suppressed the expression of EGFR, PI3K/AKT, c-MYC, P-gp, ABCG2, and the downstream cell cycle factor CDK4, but increased the expression of p53. These combined findings confirmed that VPS33B serves a tumor suppressor in OC.

miRNAs are considered as middle mediators that are involved in the signaling network of tumor pathogenesis.[26,27] miR-133a-3p is a tumor suppressor that directly targets EGFR in the pathogenesis of several tumors[28,29] except OC. Consistent with our previous reports,[11,12] miR-133a-3p directly targeted EGFR and suppressed cell growth in OC. Furthermore, miR-133a-3p inactivated the PI3K/AKT/c-Myc pathway and upregulated p53 expression in OC cells.

p53 is a classic tumor suppressor in cancer research.[30] Notably, the miR-133-3p promotor hides a p53 binding site. Transfection of the p53 plasmid induced miR-133a-3p expression. ChIP, EMSA, and luciferase activity assay demonstrated the combination of p53 with the miR-133a-3p promoter. In addition, knockdown of miR-133a-3p in OC cells with p53 plasmid transfection resulted in the upregulation of EGFR/PI3K/AKT/c-Myc signaling and downregulation of p53, which suggested that p53 regulated the EGFR/PI3K/AKT/c-Myc pathway by directly inducing miR-133a-3p expression.

c-Myc serves as an oncogene and a therapeutic target in various tumors.[31] Consistent with the previous study,[31] c-Myc suppressed p53 expression in OC. Moreover, mRNA expression of p53 was downregulated in c-Myc overexpressing OC cells, which suggested that c-Myc may suppress p53 expression at the transcriptional level. Notably, c-Myc was predicted to be a candidate potential transcription factor binding to the p53 promoter with PROMO and USCS software. Subsequently, by ChIP, EMSA, and luciferase activity assays, we demonstrated that c-Myc could directly bind to its promoter. Transfection of the p53 plasmid induced miR-133a-3p and reduced the EGFR/PI3K/AKT/c-Myc signal, which suggested that c-Myc induced miR-133a-3p and attenuated the EGFR/PI3K/AKT signals by directly suppressing p53 expression. Finally, knockdown of EGFR led to increased p53/miR-133a-3p and decreased the PI3K/AKT/c-Myc pathway. Moreover, the combination of p53 and the miR-133a-3p promoter was significantly reduced after c-Myc transfection in OC cells. These results indicated a feedback loop among EGFR, PI3K, AKT, c-Myc, p53, and miR-133a-3p.

In the present study, we found for the first time that VPS33B could regulate the EGFR/PI3K/AKT/c-Myc/p53 signal in OC. Furthermore, our study showed that overexpressed VPS33B induced miR-133a-3p expression. Transfection of EGFR significantly upregulated the PI3K/AKT/c-Myc signal and decreased the p53/miR-133a signal in overexpressed VPS33B OC cells. In addition, transfecting EGFR to VPS33B-overexpressing OC cells significantly increased the combination of c-Myc with the p53 promoter and decreased the combination of p53 with the miR-133a-3p promoter, respectively.
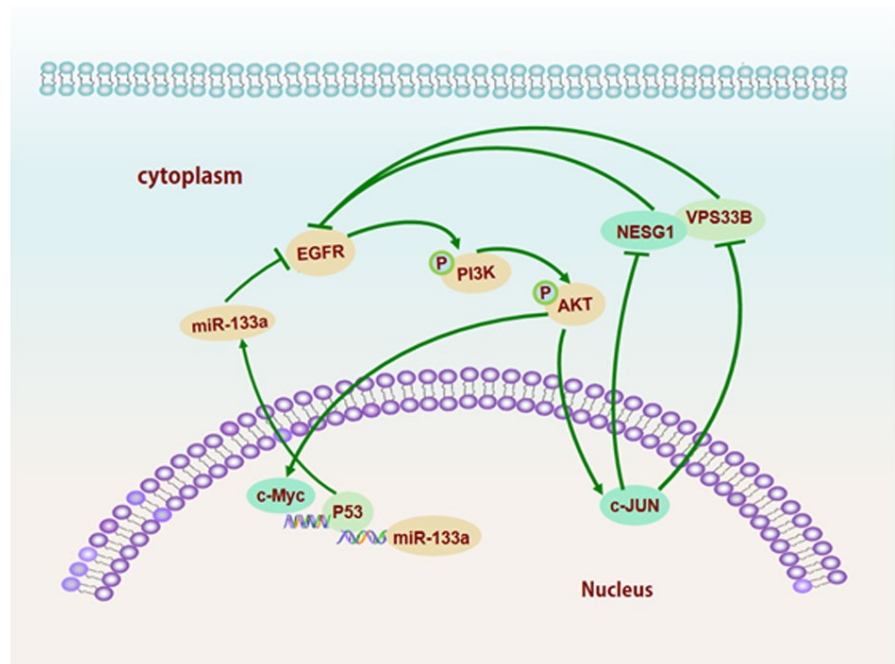

FIGURE 8 Potential signaling pathway driven by VPS33B interacting with NESG1 to suppress cell growth in OC

The combined findings demonstrated that VPS33B could regulate the EGFR/PI3K/AKT/c-Myc/p53/miR-133a-3p feedback loop.

Protein-protein interactions are important cellular signals.[32] In previous studies, we used the Y2H approach to predict the candidate interaction protein of NESG1 in 293T cells.[11] We found that VPS33B was predicted as a candidate potential interaction protein of NESG1. Furthermore, we demonstrated the interaction between VPS33B and NESG1 in OC with CoIP and confocal laser analysis. We then found that VPS33B and NESG1 have mutually stimulated expression by decreasing the PI3K/AKT signal to downregulate the expression of c-Jun, and that c-Jun was an oncogenic transcription factor that could directly bind to the VPS33B and NESG1 promotor and, therefore, suppressed the expression of both genes. Transfecting NESG1 markedly upregulated the expression of p53/miR-133a-3p and downregulated the EGFR/PI3K/AKT/c-Myc signal and its downstream CDK4. These results showed that NESG1 as a tumor suppressor could interact with VPS33B, and mediated VPS33B-induced OC suppression by regulating the EGFR/PI3K/AKT/c-Myc/p53/miR-133a-3p feedback loop.

5 | CONCLUSIONS

In summary, VPS33B functions as a tumor suppressor, which interacts with NESG1 and co-modulates the EGFR/PI3K/AKT/c-Myc/p53/miR-133a-3p feedback loop and its downstream factors (Figure 8), suppressing cell growth and cisplatin chemoresistance. Our study provides a new insight into the significance of VPS33B in OC.

CONFLICT OF INTEREST
The authors declare that they have no competing interests.

AUTHOR CONTRIBUTIONS
YXN, YF, and LYL conceived of the study and supervised and co-ordinated all aspects of the work; YXN, ZYZ, YAD and WFF designed the research, wrote the paper, and prepared figures and tables; ZYZ, YF, LH, HLL, JZL, and CZ performed experiments, interpreted data, and prepared figures and tables; and LYL and YF contributed analytical tools. All authors read and approved the manuscript.

ETHICS APPROVAL AND CONSENT TO PARTICIPATE
The Ethics Committee of the First Affiliated Hospital of Guangzhou Medical University authorized the experimental and research protocols of this study. All procedures performed in this study were according to the ethical standards of the institutional research committee and with the 1964 Helsinki declaration and its later amendments or comparable ethical standards. Written informed consent was provided and signed by all patients prior to sample collection. All experimental protocols were approved by a Cancer Center Committee of Southern Medical University. The study was reviewed and approved by the Southern Medical University animal care and use committee.

CONSENT FOR PUBLICATION
We have obtained consent from all the participants of this study to publish this paper.

DATA AVAILABILITY STATEMENT
The datasets used and/or analyzed during the current study are available from the corresponding author on reasonable request.

ORCID
Longyang Liu https://orcid.org/0000-0002-1014-3625

REFERENCES
1. Chen W, Zheng R, Baade PD, et al. Cancer statistics in China, 2015. *CA Cancer J. Clin*. 2016;66:115-132.
2. Lheureux S, Braunstein M, Oza AM. Epithelial ovarian cancer: evolution of management in the era of precision medicine. *CA Cancer J Clin*. 2019;69:280-304.
3. Mittica G, Ghisoni E, Giannone G, et al. PARP inhibitors in ovarian cancer. *Recent Pat Anticancer Drug Discov*. 2018;13:392-410.
4. Taylor KN, Eskander RN. PARP inhibitors in epithelial ovarian cancer. *Recent Pat Anticancer Drug Discov*. 2018;13:145-158.
5. Liu L, Ning Y, Yi J, et al. miR-6089/MYH9/β-catenin/c-Jun negative feedback loop inhibits ovarian cancer carcinogenesis and progression. *Biomed Pharmacother*. 2020;125:109865.
6. Weyand AC, Lombel RM, Pipe SW, Shavit JA. The role of platelets and epsilon-aminocaproic acid in arthrogryposis, renal dysfunction, and cholestasis (ARC) syndrome associated hemorrhage. *Pediatr Blood Cancer*. 2016;63:561-563.
7. Seo SH, Hwang SM, Ko JM, et al. Identification of novel mutations in the VPS33B gene involved in arthrogryposis, renal dysfunction, and cholestasis syndrome. *Clin Genet*. 2015;88:80-84.
8. Xiang B, Zhang G, Ye S, et al. Characterization of a novel integrin binding protein, VPS33B, which is important for platelet activation and in vivo thrombosis and hemostasis. *Circulation*. 2015;13:2334-2344.
9. Urban D, Li L, Christensen H, et al. The VPS33B-binding protein VPS16B is required in megakaryocyte and platelet alpha-granule biogenesis. *Blood*. 2012;120:5032-5040.
10. Wang C, Cheng Y, Zhang X, et al. Vacuolar protein sorting 33B is a tumor suppressor in hepatocarcinogenesis. *Hepatology*. 2018;68:2239-2253.
11. Liang Z, Liu Z, Cheng C, et al. VPS33B interacts with NESG1 to modulate EGFR/PI3K/AKT/c-Myc/P53/miR-133a-3p signaling and induce 5-fluorouracil sensitivity in nasopharyngeal carcinoma. *Cell Death Dis*. 2019;10:305.
12. Chen Y, Liu Z, Wang H, et al. VPS33B negatively modulated by nicotine functions as a tumor suppressor in colorectal cancer. *Int J Cancer*. 2020;146:496-509.
13. Li Z, Yao K, Cao Y. Molecular cloning of a novel tissue-specific gene from human nasopharyngeal epithelium. *Gene*. 1999;237:235-240.
14. Liu Z, Li X, He X, et al. Decreased expression of updated NESG1 in nasopharyngeal carcinoma: its potential role and preliminarily functional mechanism. *Int J Cancer*. 2011;12:2562-2571.
15. Liu Z, Chen C, Yang H, et al. Proteomic features of potential tumor suppressor NESG1 in nasopharyngeal carcinoma. *Proteomics*. 2012;12:3416-3425.

16. Liu Z, Mai C, Yang H, et al. Candidate tumour suppressor CCDC19 regulates miR-184 direct targeting of C-Myc thereby suppressing cell growth in non-small cell lung cancers. *J Cell Mol Med*. 2014;18:1667-1679.

17. Lin X, Zuo S, Luo R, et al. HBX-induced miR-5188 impairs FOXO1 to stimulate β-catenin nuclear translocation and promotes tumor stemness in hepatocellular carcinoma. *Theranostics*. 2019;9:7583-7598.

18. Liu Y, Jiang Q, Liu X, et al. Cinobufotalin powerfully reversed EBV-miR-BART22-induced cisplatin resistance via stimulating MAP2K4 to antagonize non-muscle myosin heavy chain IIA/glycogen synthase 3β/β-catenin signaling pathway. *EBioMedicine*. 2019;48:386-404.

19. Li Y, Liu X, Lin X, et al. Chemical compound cinobufotalin potently induces FOXO1-stimulated cisplatin sensitivity by antagonizing its binding partner MYH9. *Signal Transduct Target Ther*. 2019;4:48.

20. Liu C, Peng X, Li Y, et al. Positive feedback loop of FAM83A/PI3K/AKT/c-Jun induces migration, invasion and metastasis in hepatocellular carcinoma. *Biomed Pharmacother*. 2020;123:109780.

21. Lin X, Li AM, Li YH, et al. Silencing MYH9 blocks HBx-induced GSK3β ubiquitination and degradation to inhibit tumor stemness in hepatocellular carcinoma. *Signal Transduct Target Ther*. 2020;5:13.

22. Zou Y, Lin X, Bu J, et al. Timeless-stimulated miR-5188-FOXO1/β-catenin-c-jun feedback loop promotes stemness via ubiquitination of β-catenin in breast cancer. *Mol Ther*. 2020;28:313-327.

23. Qiu M, Xue C, Zhang L. Piperine alkaloid induces anticancer and apoptotic effects in cisplatin resistant ovarian carcinoma by inducing G2/M phase cell cycle arrest, caspase activation and inhibition of cell migration and PI3K/Akt/GSK3β signalling pathway. *J BUON*. 2019;24:2316-2321.

24. Yin X, Yang G, Ma D, et al. Inhibition of cancer cell growth in cisplatin-resistant human oral cancer cells by withaferin-A is mediated via both apoptosis and autophagic cell death, endogenous ROS production, G2/M phase cell cycle arrest and by targeting MAPK/RAS/RAF signalling pathway. *J BUON*. 2020;25:332-337.

25. Tiemin P, Fanzheng M, Peng X, et al. MUC13 promotes intrahepatic cholangiocarcinoma progression via EGFR/PI3K/AKT pathways. *J Hepatol*. 2020;72:761-773.

26. Deng X, Liu Z, Liu X, et al. miR-296-3p Negatively Regulated by Nicotine Stimulates Cytoplasmic Translocation of c-Myc via MK2 to Suppress Chemotherapy Resistance. *Mol Ther*. 2018;26:1066-1081.

27. Zhao M, Xu P, Liu Z, et al. Dual roles of miR-374a by modulated c-Jun respectively targets CCND1-inducing PI3K/AKT signal and PTEN-suppressing Wnt/β-catenin signaling in non-small-cell lung cancer. *Cell Death Dis*. 2018;9:78.

28. He B, Lin X, Tian F, et al. MiR-133a-3p Inhibits Oral Squamous Cell Carcinoma (OSCC) Proliferation and Invasion by Suppressing COL1A1. *J Cell Biochem*. 2018;119:338-346.

29. Cui W, Zhang S, Shan C, et al. microRNA-133a regulates the cell cycle and proliferation of breast cancer cells by targeting epidermal growth factor receptor through the EGFR/Akt signaling pathway. *FEBS J*. 2013;280:3962-3974.

30. Navalkar A, Ghosh S, Pandey S, et al. Prion-like p53 amyloids in cancer. *Biochemistry*. 2020;59:146-155.

31. Allen-Petersen BL, Sears RC. Mission possible: advances in MYC therapeutic targeting in cancer. *BioDrugs*. 2019;33:539-553.

32. Li Q, Yang Z, Zhao Z, et al. HMNPPID-human malignant neoplasm protein-protein interaction database. *Hum Genomics*. 2019;13:44.

SUPPORTING INFORMATION

Additional supporting information may be found online in the Supporting Information section.